HIGH RESOLUTION SIMULATION OF A VACUUM MICRODIODE

June 2012

Pálmar Jónsson
Master of Science in Electrical Engineering

HIGH RESOLUTION SIMULATION OF A VACUUM MICRODIODE

Pálmar Jónsson
Master of Science
Electrical Engineering
June 2012
School of Science and Engineering
Reykjavík University

M.Sc. RESEARCH THESIS

ISSN 1670-8539

High resolution simulation of a vacuum microdiode

by

Pálmar Jónsson

Research thesis submitted to the School of Science and Engineering
at Reykjavík University in partial fulfillment of
the requirements for the degree of
Master of Science in **Electrical Engineering**

June 2012

Research Thesis Committee:

Dr. Andrei Manolescu, Supervisor
Professor, Reykjavík University

Dr. Ágúst Valfells, Supervisor
Associate Professor, Reykjavík University

Dr. Sigurður Ingi Erlingsson, Examiner
Associate Professor, Reykjavík University

The undersigned hereby certify that they recommend to the School of Science and Engineering at Reykjavík University for acceptance this research thesis entitled **High resolution simulation of a vacuum microdiode** submitted by **Pálmar Jónsson** in partial fulfillment of the requirements for the degree of **Master of Science** in **Electrical Engineering**.

_____

Date

_____

Dr. Andrei Manolescu, Supervisor
Professor, Reykjavík University

_____

Dr. Ágúst Valfells, Supervisor
Associate Professor, Reykjavík University

_____

Dr. Sigurður Ingi Erlingsson, Examiner
Associate Professor, Reykjavík University

High resolution simulation of a vacuum microdiode

Pálmar Jónsson

June 2012

Abstract

In this thesis a vacuum microdiode is simulated where each electron in the system is regarded as point charge and observed through the system from Cathode to Anode. A space charge limited emission process is simulated. Low voltage sufficies to create large electric field across the vacuum diode since the gap spacing is kept in the micrometer region. A Fourir analysis on the emission and absorption process is presented. A simulation with the same parameters as earlier research [7] is presented as well as expanding the simulation parameters and mapping the response to different combinations of input parameters.
Finally two variations of the initial experiment where initial kinetic energy is introduced corresponding to the operating temperature of the diode.

Hermun á míkró díóðu í lofttæmi með hárri upplausn

Pálmar Jónsson

Júní 2012

Útdráttur

Hermun á míkró díóðu í lofttæmi þar sem hver rafeind er talin sem punkhleðsla er fylgt frá Catóðu til Anódu. Ytra rafsvið veldur kröftum sem draga rafeindir inn í kerfið. Fjöldi rafeinda í kerfinu takmarkast af mettun Catóðu sem gerist þegar fjöldi rafeinda í kerfinu veldur rafkröftum jöfnum þeim sem ytra rafsvið veldur. Þar sem stærð díóðunar er lítil dugar lág spenna til að búa til sterkt rafsvið. Fourier tíðnigreining sýnir tíðnir sem koma fram í díóðunni. Niðurstöður eru bornar saman við fyrri rannsóknir auk þess sem reynt er að kortleggja hegðun við mismunandi stærð og spennu. Þess næst eru skoðuð tilfelli með upphafshraða og loks er fyrsta hermunin endurtekin með lægra tímaskrefi og hærri upplausn.

Contents

List of Figures

List of Tables

Chapter 1

Introduction

Vacuum tubes were introduced in the early 20th century and later used to build rectifiers, amplifiers, switches and oscillators, to name a few applications. Until the introduction of the transistor and other solid-state devices in the mid 20th century vacuum devices were dominant in electronics. Due to advantages with regard to miniaturization and manufacturing costs solid-state electronics have become the standard, except for special applications, e.g. high-power and high frequency where vacuum electronics are preferable [2, 5, 9]. Today's production technology enables building devices in the micrometer region and opens up the possibility to create smallar more compact microelectronics that don't require the high voltages used in earlier designs of vacuum devices.

The cost of simulating a system increases exponentally with the number of particles in a system and several methods have been developed to try to mitigate the computational cost of detailed simulations with simplifications and grouping or clustering. A well known method for simulations is called „Particle in Cell" (PIC). This method is implemented by partitioning the space of concern to a number of cells and counting the number of particles in each cell as well as finding the center of mass. This center of mass is called a macro-particle and has charge equal to the number of particles in the cell time the charge of the particles, assuming they all have the same charge. This knowledge is then used to find electric potentials at grid points according to the placement of macro-particles in the cell and from there the electric field and finally forces acting upon the macro-particles are calculated. This method can be made very fast by limiting the number of cells at cost of accuracy. This method has the advantage of relatively few calculations needed compared to calculating forces between each and every particle seperately but introduces errors in calculations. In particular short-range Coulomb effects and scattering are obscured [3, 6].

In this thesis a more accurate approach to diode simulation is presented where each electron in the system is tracked from cathode to anode. This is possible due to the extremly small dimension of the system so the number of particles doesn't grow out of hand and can be kept track of individually resulting in high resolution simulation.

This thesis will start with a description of the physical model. Then focus on how the simulations were performed, i.e. how the computer program simulating the device was constructed and analyzed and a little about the pros and cons of different programming languages.

Then a presentation of results for varius combinations of input parameters with and without initial velocity as well as a comparison with earlier research done by Pedersen et al. [7].

Chapter 2

Model

The system consists of a simple planar vacuum diode, shown in Figure 2.1. The outer wall is omitted but the main components of concern are shown, at the top the circular cathode which emits electrons. The cathode has a thickness of 1 nm and radius R. The anode at the bottom absorbs electrons. The electrodes are seperated by a vacuum gap, d, and the potential difference is V. The applied electric field is uniform and parallel to the z-axis.

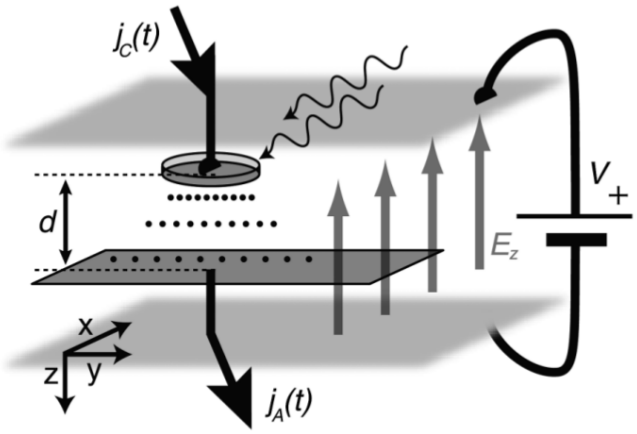

Figure 2.1: A diagram of the system simulated. Electrons are accelerated from the cathod (top) towards the bottom of the system (anode). [7]

2.1 Physical Model

An external electric field is used to accelerate electrons from the cathode towards the anode. The field is considered constant everywhere in the system. The electrons are emitted using a laser shining on the cathode and relying on photoelectric emission. As more electrons are emitted into the system the net electric field at the cathode which is due to the external electric field and that of the electrons starts to decrease until the number of electrons emitted is great enough to reverse the field where electrons are emitted. Emission is

space-charge limited meaning that emission continues until enough electrons are emitted so that the net electric force at the cathode becomes zero. Then the external electric field is equal to the electric field created by the electrons in the system. Another option is to have the emission source limited. That way there is a limit of available electrons released at the cathode in each iteration and only N electrons can be emitted at each iteration. This thesis is concerned with the space-charge limited regime.

2.2 Computational Algorithm

Since the program is to be used as a research tool for other people it needs to be clearly written and easy to understand so it can easily be run for other scenarios. Algorithm 1 shows a pesudo code of how it is constructed. The implementation of these functions is not shown but explained in later chapters.

Algorithm 1 Flow of the program

```
Initialize program variables
while (Conditions true) do
    Add electrons to system
    Calculate forces in system
    Move electrons
    Check boundary conditions
    Save data (Positioning at each iteration) [Optional - Potentially slow]
end while
Save data (Escape vectors)
```

C++ was chosen for the simulation and Python for the data analysis.

The easiest way to program was to create a class with vectors which keep track of positions, escaped electrons and force, to name a few parameters, and all functions belong to this class. Thus calling a function to move the electrons is easy and there is no need to supplement any variables to the function. This means that all functions and variables of this class can be accessed by using the dot operator. Usually functions are seperate entities and have to be supplemented with input variables and return output variables but using the class method complex functions which require much input data are extremely simple to call.

2.2.1 Emission

Random Distribution Algorithm

Normally a program like this has a huge number of particles [3] and needs sophisticated random number generating algorithm which produces a long sequence of apparently random results. In this simulation the number of electrons is so small that almost any algorithm should do. The one used is from technical enhancements to the C++ library.

Circular Distribution

When injecting electrons into the system they're placed randomly on a circle with radius of $250[nm]$ and $1[nm]$ below the surface of the cathode. This is done by choosing two random numbers from a uniform distribution, one corresponding to radius and the other to angle. To make sure that the area distribution is the same everywhere on the cathode care must be taken when assigning the raidal position. Each radial segment extending from r_i to r_{i+1} must be of the same size as any other. Thus

$$\int_{r_0}^{r_1}\int_{0}^{2\cdot\pi} r\cdot dr\cdot d\theta = \int_{r_1}^{r_2}\int_{0}^{2\cdot\pi} r\cdot dr\cdot d\theta \tag{2.1}$$

and subsequently

$$\begin{aligned} r_2^2 &= 2\cdot r_1^2 - r_0^2 \\ r_3^2 &= 2\cdot r_2^2 - r_1^2. \end{aligned} \tag{2.2}$$

By continuing with this method and realizing that r_0 is just the center, equal to zero, a formula for the n-th radius is given by

$$r_n^2 = n\cdot r_1^2 \tag{2.3}$$

Another observation is that r_N is the outer radius of the emitter, equal to $250[nm]$ in this case. Thus

$$r_1 = \frac{r_N}{\sqrt{N}} \tag{2.4}$$

Substituting Equation (2.4) into Equation (2.3) and using the knowledge that $r_N = 250[nm]$ gives

$$r_n = \frac{\sqrt{n}}{\sqrt{N}}\cdot r_N \qquad n = 1, 2, ..., N-1, N. \tag{2.5}$$

The fraction above, n/N, is a random variable in the interval $[0, 1]$ which is chosen from a uniform random distribution and the square root taken of that number and that is the radius used. This method ensures that the area density of electrons is constant everywhere on the surface of the cathode. Figure 2.2 shows the view of the x-y plane after first iteration as well as a outline of the surface of the cathode.

With the radial length calculated the angular position is a random number uniformly distributed in the range $[0, 2\pi]$.

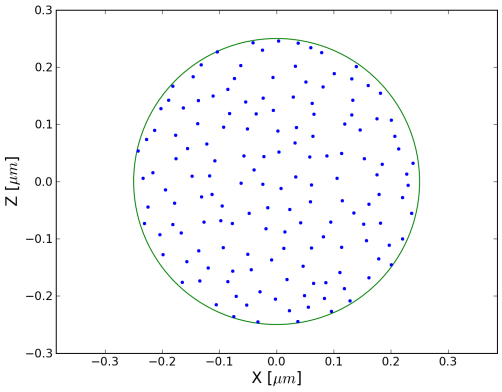

Figure 2.2: Distribution of electrons over the Cathode at the first iteration. Cathode surface shown as circle. View of the x-y plane.

Initial Positioning

When injecting a new electron into the system a random position is generated in the x-y plane. Then the electron is placed $1[nm]$ below the surface of the diode, at z-position $-1[nm]$, and the forces which act upon each electron are calculated. If the sum of the forces act in the positive z-direction, so that the electron is accelerated into the system, then it is injected at z-position of $1[nm]$. Otherwise it's removed and the process starts again until 100 unsuccessful attempts in a row are registered. Then the cathode is considered saturated and the system is evolved one timestep. If an electron has 99 failed attempts but is successfully injected at attempt 100 then this counter is reset to zero. That is the counter is not cumulative for all electrons. The reason why $1[nm]$ is chosen is that the cathode is considered to have some thickness and $1[nm]$ to be the surface of the cathode.

Initial Velocity and Movement Equation

The kinetic energy of an electron travelling through the system can be stated directly in terms of the voltage applied. If the difference in voltage from cathode to anode is $2[V]$ the maximum energy of an electron going from the cathode to the anode is equal to $E = 2[eV]$ [8]. The program can calculate a position, x_{i-1}, so that any percentage of this maximum energy can be chosen as initial energy. The derivations follows. The equation

for kinectic energy is

$$E = \frac{1}{2} \cdot m \cdot v^2 \tag{2.6}$$

where E and m are known values for kinetic energy and mass of an electron respectively. Then

$$v = \sqrt{\frac{2 \cdot E}{m}}. \tag{2.7}$$

The velocity is calculated from current and former position and the timestep which can be written as

$$v = \frac{x_i - x_{i-1}}{\Delta t} \tag{2.8}$$

where v is the velocity, x_i is the position at iteration i and Δt is the timedifference between iterations. By substituting Equation (2.8) in Equation (2.7) and simplifying the result is

$$x_{i-1} = x_i - \sqrt{\frac{2 \cdot E}{m}} \cdot \Delta t \tag{2.9}$$

where all the variable on the right side are known, x_i being the newly calculated position on the cathode.

Equation (2.9) isn't yet in its final form. In this form each electron would have the same initial speed. To have random initial velocity modification was done by adding a random variable in the range $[0, 1]$ as a multiplication to the last term in Equation (2.9). The random term is shown as $r(0, 1)$ indicating the range of value the random variable can be at. There are two ways of doing this having either uniform energy distribution or uniform velocity distribution.

Equation (2.10) shows the uniform velocity distribution,

$$x_{i-1} = x_i - \sqrt{\frac{2 \cdot E}{m}} \cdot \Delta t \cdot r(0, 1). \tag{2.10}$$

Equation (2.11) shows the uniform energy distribution,

$$x_{i-1} = x_i - \sqrt{\frac{2 \cdot E \cdot r(0, 1)}{m}} \cdot \Delta t. \tag{2.11}$$

Temperature and Initial Velocity

The temperature of the system plays a vital role in simulations. The Boltzmann distribution gives the energy of a system as $k \cdot T$. For electrons to be emitted with 1% of the

maximum final kinetic energy the temperature of the system can be estimated by

$$k \cdot T = KE \tag{2.12}$$

where k is the Boltzmann constant in $\left[\frac{eV}{K}\right]$, K is the temperature of the system in $[K]$ and KE is the fraction of the maximum final energy in $[eV]$. Putting in values for h and KE and solving for T the temperature is

$$T = \frac{0.01[eV]}{8.62 \cdot 10^{-5}[eV/K]} = 116[K]. \tag{2.13}$$

On the more familiar Celsius temperature scale this equals $-157[^{\circ}C]$ so some kind of liquid cooling system would have to be used. If the diode were to be operated at room temperature of $20[^{\circ}C]$ then the maximum initial kinetic energy of the electrons is $0.48[eV]$. Such an extreme scenario was not simulated. For comparison liquid Nitrogen has a boiling point of $77[K]$ $(-196[^{\circ}C])$

2.2.2 Force Calculation

There are two seperate forces acting upon electrons in the diode. One is due to static electric field and the other one is due to Coulumb forces between electrons.

Uniform External Electric Field

There is a fixed potential over the whole diode. This yields a electric field of

$$E = \frac{V}{d}, \tag{2.14}$$

where d is the gap spacing and V the voltage at the anode.

This field affects the electrons in the system by linear relations,

$$F = q \cdot E. \tag{2.15}$$

Coulumb Forces

The electric field due to a single electron is given by

$$\vec{E} = \frac{q_e}{4 \cdot \pi \cdot \epsilon \cdot r^2}\hat{r} \tag{2.16}$$

where r is the distance to the point of measure.

The force acting upon another electron is

$$\vec{F} = \frac{q_e^2}{4 \cdot \pi \cdot \epsilon \cdot r^2}\hat{r}, \tag{2.17}$$

which is the result of substituting Equation (2.16) into Equation (2.15).

In these equations $\epsilon = \epsilon_0 \cdot \epsilon_r$ is the permittivity of the medium. Since vacuum is considered to be inside the diode the relative permittivity, ϵ_r is equal to 1 and therefor $\epsilon = \epsilon_0$. In these equations r is the distance between two electrons given by

$$r = \sqrt{(\Delta x)^2 + (\Delta y)^2 + (\Delta z)^2}. \tag{2.18}$$

The x,y and z components of the force are calculated by multiplying the force equation with $\frac{\Delta x}{r}$ resulting in the following equation

$$F_x = \frac{q_e^2}{4 \cdot \pi \cdot \epsilon \cdot r^2} \cdot \frac{\Delta x}{r} = \frac{q_e^2 \cdot (x_2 - x_1)}{4 \cdot \pi \cdot \epsilon \cdot \left[(x_2 - x_1)^2 + (y_2 - y_1)^2 + (z_2 - z_1)^2\right]^{3/2}} \tag{2.19}$$

which is used for the three Cartesian dimensions used in all calculations.

2.2.3 Equations of Motion

The Verlet algorithm is calculated using a Taylor expansion for position at time x_{t-i} and x_{t+i} and adding the equations and simplify [4]

$$\begin{aligned} \vec{x}_{i+1} &= \vec{x}_i + \vec{v}_i \cdot \Delta t + \tfrac{\vec{a}_i \cdot (\Delta t)^2}{2} + \text{Higher order terms} \\ \vec{x}_{i-1} &= \vec{x}_i - \vec{v}_i \cdot \Delta t + \tfrac{\vec{a}_i \cdot (\Delta t)^2}{2} + \text{Higher order terms}, \end{aligned} \tag{2.20}$$

resulting in

$$x_{i-1} + x_{i+1} = 2 \cdot x_i + a_i \cdot (\Delta t)^2, \tag{2.21}$$

neglecting higher order terms. In this form the only variable which hasn't been accounted for is the acceleration, a. Newton's second law states that

$$F = m \cdot a \rightarrow a = \frac{F}{m} \tag{2.22}$$

where F was calculated by the methods shown in the force calculations section and m is the mass of an electron, $m_e = 9.11 \cdot 10^{-31}[kg]$. Substituting Equation (2.22) into

Equation (2.21) and rearranging gives the form used in calculations of new position

$$x_{i+1} = 2 \cdot x_i - x_{i-1} + \frac{F}{m} \cdot (\Delta t)^2. \tag{2.23}$$

2.2.4 Absorption

The only ways electrons are removed from the system is if they exceed the system boundaries at cathode or anode. The system dimensions are assumed to be such that the sides have no effect on the system and since the external electric field is considered uniform everywhere in the anode they all escape at anode or cathode eventually.

Anode

This is where the majority of electrons escape the system from. They cross the system and are absorbed at the anode and that is the normal operation of the diode. The electrons aren't absorbed instantaneously and Section 2.2.5 in Section 2.2.5 discusses method used to simulate absorption spread over time.

Cathode

A very small part of the electrons are pushed back into the cathode because of Coulumb forces. When injecting electrons into the system an test electron is placed at position $= z = -1[nm]$ and forces acting on her calculated. If they act to accelerate her into the system she's injected at the same x and y coordinates but on the surface of the cathode at $z = 1[nm]$. It is possible that there is another electron extremly close to that position. This causes extreme Coulumb forces between these electrons pushing the one closer to the cathode back into it. This is an extreme case and the total number of electrons escaping this way is insignificant.

Both anode and cathode are considered perfectly flat.

2.2.5 Data Analysis

After a single simulation the following steps are taken in data analysis.

Acquisition

As shown in Algorithm 1 there are two ways to save the data. One method saves data after each iteration and keeps track of three dimensional position in CSV format, comma seperated values. This makes it possible to visualize the distribution after the first emission process to verify that the area distribution is correct and also make a video of the system to see how it behaves. This method is optional because accessing the hard disk drive in every iteration dramatically slows down simulations.
The second method, which is run after the main program loop, saves one vector which is as long as there are many iterations. Each element in this vector holds a count of how many electrons escape at each iteration. The index of the vector corresponds to the iteration at which the electrons escaped the system.

Filtering

The charge of the electrons isn't absorbed by the boundaries all at once but spread over time. A Gaussian smoothing curve is convoluted with the data to represent the charge being absorbed over time. The only parameters of this smoothing function which need to be determined are the standard deviation of the curve, σ, and how wide the the curve should be. Since about 99.7% of the data in a Gaussian distribution lies within three standard deviations from the mean, the width of the smoothing function is chosen to be six time the standard deviation and not changed for the remainder of this thesis. That equals three standard deviations in each direction from the center which accounts for the 99.7%. This smoothing function is convoluted with the raw data for emission and absorption resulting in smooth curves. It should be noted that a wide smoothing function removes very high frequency components from the signal but they've been observed to be mearly a fraction of the amplitude of the largest peaks which have always had frequencies which are lower than $2.5[THz]$. The magnitude of the smoothing function is normalized to one although that doesn't result in the area of the distribution to equal one. The magnitude scale is arbitrary in this thesis and only the frequencies are of interest. Note that fourier analysis plots will show the x-axis go up to $2.5[THz]$ or $[3.5[THz]$ but the different cutoffs are not significant to the readers understanding of what's happening in the figures.

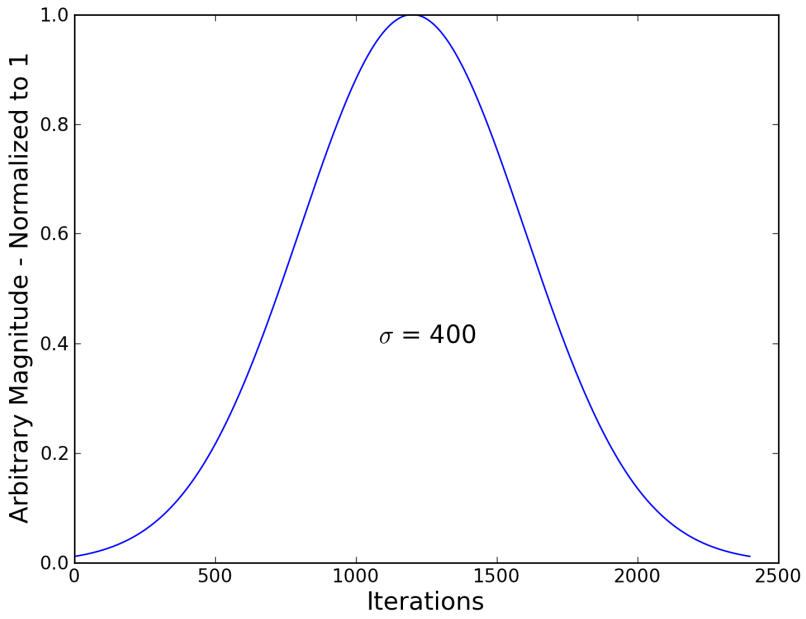

Figure 2.3: Gaussian bell curve to be convoluted with raw data.

For the remainder of this thesis all data is smoothed using the following parameters, shown in Table 2.1, in the Gaussian smoothing function, Figure 2.3.

	Emission		Absorption	
σ	$800[iter]$	$800[fs]$	$400[iter]$	$400[fs]$
Total width	$4800[fs]$ (iter)	$4800[fs]$	$2400[iter]$	$2400[fs]$

Table 2.1: Parameters for smoothing function. One iteration corresponds to one timestep which is one femtosecond. Both are shown as they are interchangeable.

To justify the size of the filter the de Broglie wavelength and final velocity of an electron are calculated and the time it takes an electron to travel the distance of one de Broglie wavelength. The de Broglie wavelength is defined as [8, p. 1494]

$$\lambda[nm] = \frac{h}{p} = \frac{h \cdot c}{p \cdot c} \tag{2.24}$$

where $h \cdot c \simeq 1240[eV \cdot nm]$ and $p \cdot c = \sqrt{2 \cdot K \cdot m_0 \cdot c^2}$ with K being the kinetic energy, m_0 the mass of the electron and c the speed of light in vacuum. The reason for multiplying in Equation (2.24) is to get familiar and widely known values. Substitution and simplification results in

$$\lambda[nm] = \frac{1.23[eV \cdot nm]}{\sqrt{K[eV]}}. \tag{2.25}$$

The final velocity of an electron in the system is given by

$$v = \sqrt{\frac{2 \cdot e \cdot \varphi}{m}} \tag{2.26}$$

where φ is the voltage difference between cathode and anode and e is the magnitude of the charge of an electron. Realizing that $\varphi[J] = K[eV]$, simplification results in

$$v = 593044 \cdot \sqrt{K[eV]}[m/s]. \tag{2.27}$$

Then the time, τ, it takes the electron to travel one de Broglie wavelength is

$$\tau = \frac{\lambda}{v} = \frac{1.23 \cdot 10^{-9}/\sqrt{K[eV]}}{593044 \cdot \sqrt{K[eV]}} \left[\frac{m}{m/s}\right] \approx \frac{2}{K[eV]}[fs]. \tag{2.28}$$

where K is in $[eV]$. Thus, for $K = 1[eV]$, we see that the value of σ amounts to the time taken to span hundreds of de Broglie wavelengths whereas the frequencies observed correspond to periods at two orders of magnitude greater than σ for $K = 1[eV]$.

Fourier Analysis

The data from simulations is just a count of how many electrons escape in each iteration and is represented by integers, see Figure 3.1. Since the charge of an electron absorbed by a metal surface isn't absorbed all at once but over some time a Gaussian smoothening function is convoluted with the data to produce a graph of electrons absorbed versus iteration, see Figure 3.2.This makes it possible to do a fourier analysis on the data and determine the frequency components present in the signal. After many iterations and tuning of the Fourier analysis it became apparent that no frequencies, of any importance, over $3.5[THz]$ are present so every graph of the fourier transform shows a frequency scale from zero to $3.5[THz]$. This way the relevant data is easier to identify.

The way the data is presented to the Fourier analysis if of great importance. If the data has $\bar{x} > 0$, where $\bar{x}$ is the mean of the signal, then the the first value in the analysis will be large and quite possibly much larger than the actual frequencies present in the signal and can be thought of as a DC-component in the signal. To understand this the equation for the discrete Fourier Analysis is shown in Equation 2.29,

$$F[k] = \sum_{n=0}^{N-1} x_n \cdot e^{-i \cdot 2 \cdot \pi \cdot \frac{k}{N} \cdot n}, \quad k = 0, 1, ..., N-2, N-1 \tag{2.29}$$

When calculating the first term, $F[0]$, the exponent of e is always zero so the first value is the sum of all values in the signal. This value can get quite large if the mean is large or the signal has a large number of elements. To get rid of this unwanted behaviour the mean of the signal vector is subtracted from each value before applying the Fourier analysis so the result shows the frequency components present in the signal but not this unwanted artifact,

$$F[k] = \sum_{n=0}^{N-1} (x_n - \bar{x}) \cdot e^{-i \cdot 2 \cdot \pi \cdot \frac{k}{N} \cdot n}, \quad k = 0, 1, ..., N-2, N-1 \tag{2.30}$$

where $\bar{x}$ is the mean of the signal. To further illustrate this point Figure 2.4 shows the difference between synthetic signal constructed from two sinusoids with frequencies $10[Hz]$ and $23.75[Hz]$ plus a constant to simulate a mean larger than zero and white noise.

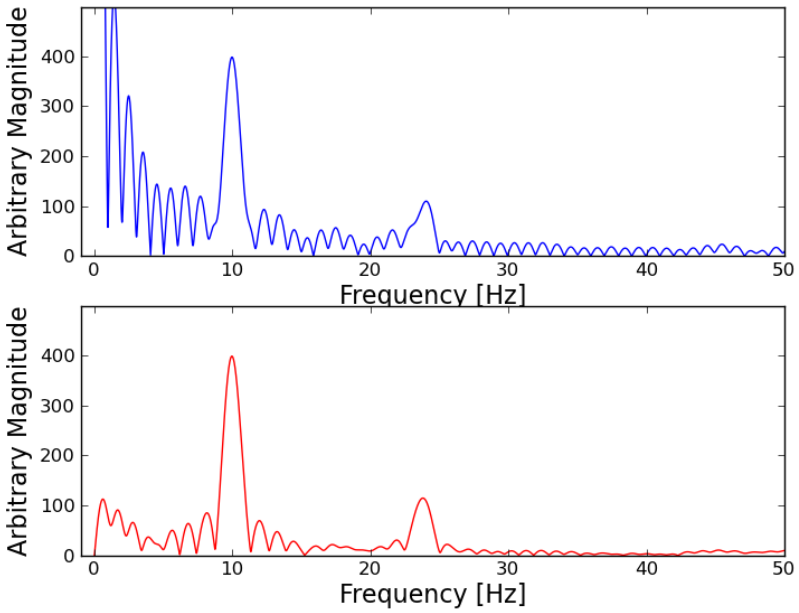

Figure 2.4: Comparison of Fourier analysis. Top plot uses Equation (2.29) while the bottom subtracts the mean as shown in Equation (2.30).

A built in function of the Numpy package[1] was used to calculate the transform while the frequency axis (x-axis) was built using as many elements as are present in the signal in the range from 0 to half the sampling frequency. The frequency component at $23.75[Hz]$ has about the same magnitude as the noise in the beginning of the signal but is much better defined as a peak. This is due to the way the signal is constructed where the sinusoid with the higher frequency has much lower amplitude that the lower frequency component. Therefor the magnitude of the noise in the signal is comparable to the low amplitude frequency component although the shape of the higher frequency component is much more definite.

Chapter 3

Results

Many different combinations of the parameters V and D were simulated but the case where $V = 1[V]$ and $d = 2[\mu m]$ will be presented to be able to compare results with research done earlier[7].

3.1 Emission

The emission process shows that the electron emission is somewhat clustered, almost as if there are sheets being discretely emitted. The reason for this is that in the beginning the system is almost empty (only empty for the first try) and Columb forces are negligible. After the system gets saturated it's evolved one timestep and further emission is attempted. Until the first „sheet" of electrons has moved a certain distance away from the cathode only few electrons are emitted. Once the first sheet crosses this distance the net electric field at the cathode acts in a direction so that more electrons are drawn into the system giving rise to the second sheet. After few iterations of this process the injection process starts to take place over a wider range of iterations although it never comes close to being so that it can be called continous, it is always pulsed. Figure 3.1 shows the raw data of the injected electrons.

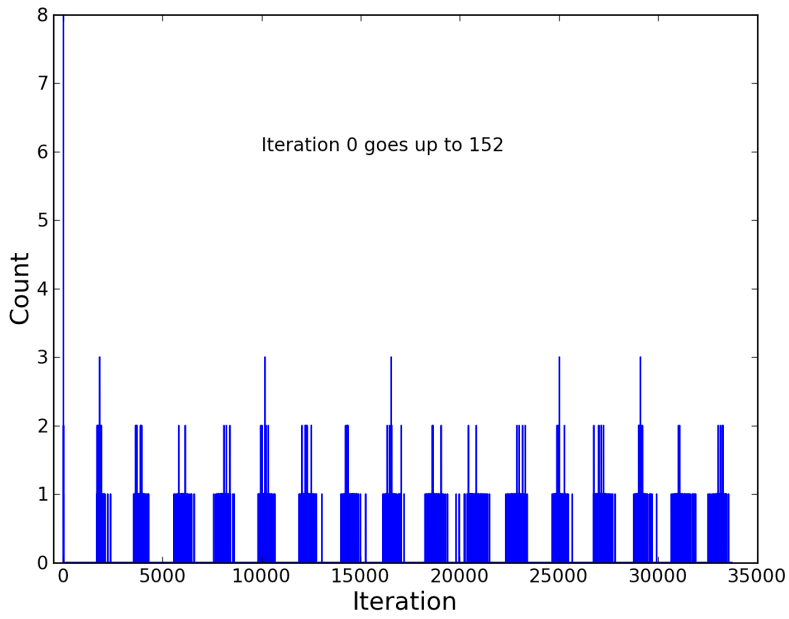

Figure 3.1: Raw Emission Data. Transient response dies out quickly and steady state is reached at around 5000 iteration.

The beginning of Figure 3.1 shows an unusually large peak at iteration 0 and the x-axis has been modified so that this peak can be seen as data but not part of the frame of the figure. This is because there are no electrons in the system at the beginning and therefor no blocking effects because of Coulumb forces by other electrons so a large number of electrons is emitted at the beginning. This behaviour does not continue in later emissions.

The data resulting from convoluting the emitted data with the Gaussian smoothing function is shown in Figure 3.2. The figure's x-axis is changed to show the first iteration more clearly.

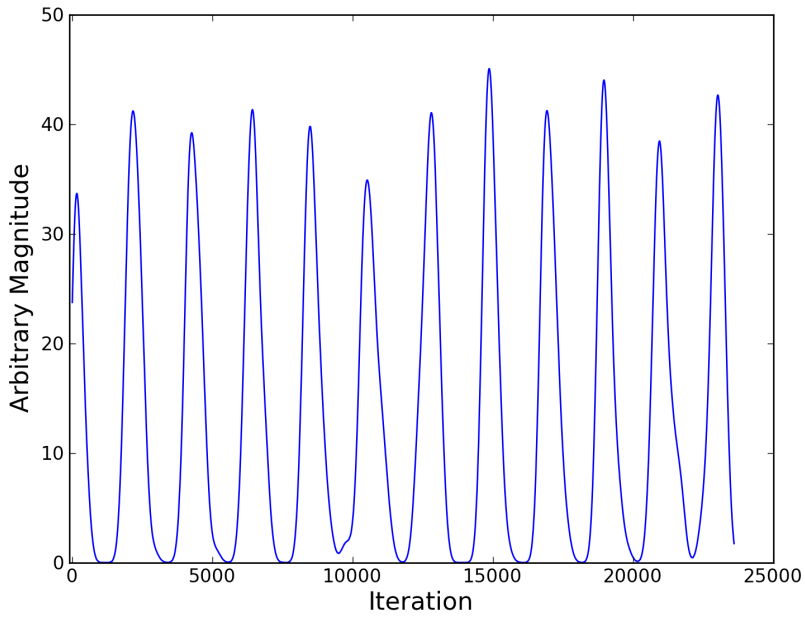

Figure 3.2: Smoothened emission. The result of convoluting the smoothing filter, Figure 2.3, with the raw from Figure 3.1

As is apparent from this data the emission is pulsed. Looking at Figure 3.2 the spacing between tops seems to be around 2000 iterations. Eight tops in the interval $[0 - 15000]$. That corresponds to a frequency of $\frac{7}{15000[iter] \cdot 10^{-15} \frac{s}{iter}} = 0.47[THz]$. To confirm this observation in a mathematical fashion a Fourier analysis is done and the results shown in Figure 3.3.

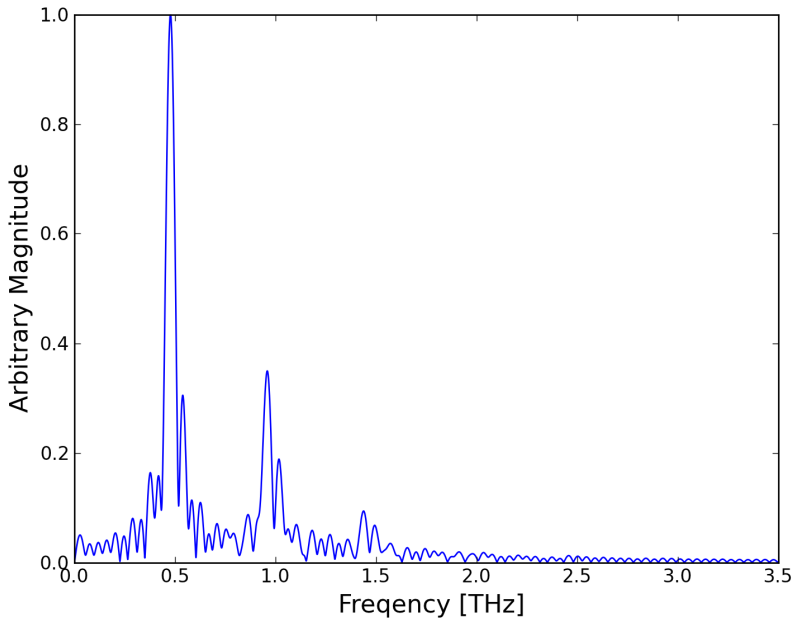

Figure 3.3: Fourier analysis on smoothened emission data. The dominant peak is at $0.5[THz]$ as calculations on data from Figure 3.2 suggested.

The results of the Fourier analysis show that the main frequency components in the system are about $0.47[Thz]$. The very high frequency components are lost when the raw data is convoluted with the smoothing function but as a comparison a fourier analysis on the raw data gives the results shown in Figure 3.4. It is not clear at this time whether the peaks at $1[THz]$ and $1.5[THz]$ are numerical artifacts or true harmonics.

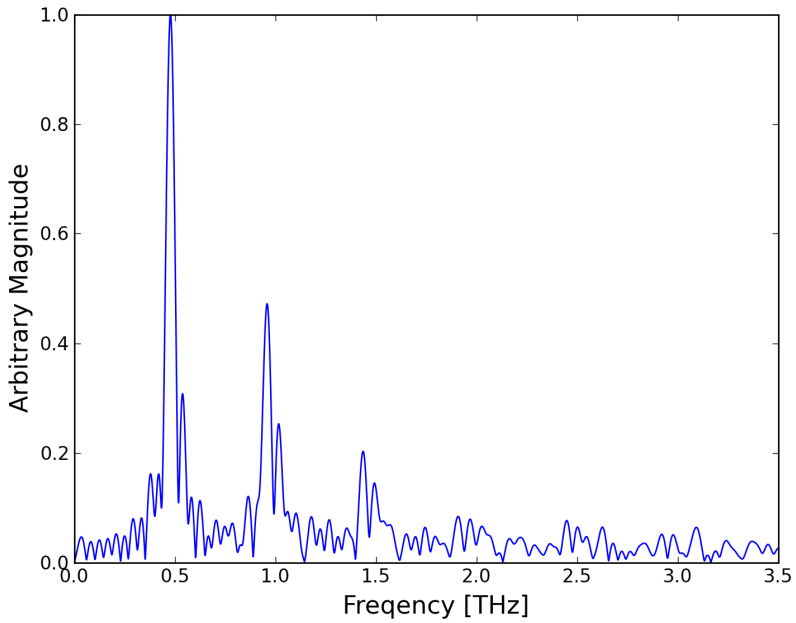

Figure 3.4: Fourier analysis on raw data

Comparison between Figures 3.3 and 3.4 shows the same peak but the latter shows a stronger high frequency components.

3.2 Absorption

Although the emission process shows that the system behaves the way it is expected it doesn't really matter so much for the function of the diode. The absorption however shows whether the diode could be useful as a high frequency generator. Figure 3.5 shows a zoom in on the smoothened absorped data.

The first peak of Figure 3.1 doesn't show up as data has been discarded so that the fluctuations in the beginning don't show up in the analysis of the steady state of the diode.

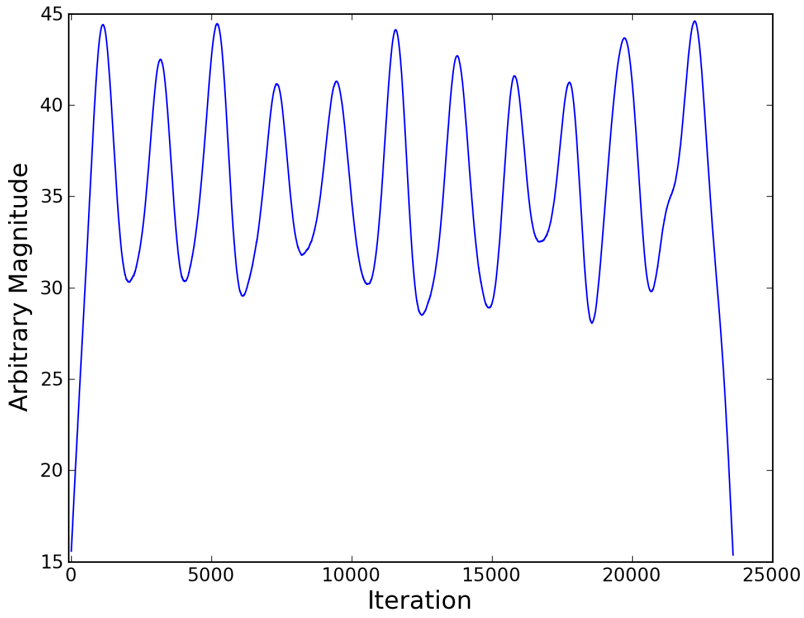

Figure 3.5: Absorped smoothened data

Fourier analysis of this data shows the frequencies present in the signal. Figure 3.6 shows a dominant frequency at $\approx 0.5[THz]$ and smaller spikes around it. The ratio of the dominant frequency against the second highest is 2.6 whether the data presented is used directly or an upper envelope constructed and analyzed. The width is $0.049[THz]$ to $0.093[THz]$, centered around $0.48[THz]$.

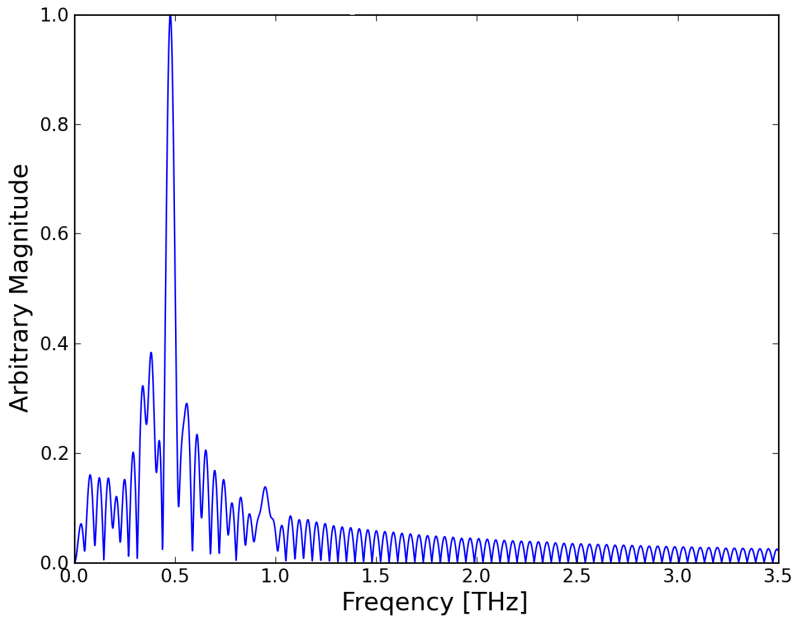

Figure 3.6: Fourier results of the absorped smoothened data

As a comparison of the frequency response a Fourier analysis of the raw data is shown in Figure 3.7. What's obvious is that the low frequency components are almost identical while the raw data analysis has many small peaks at higher frequencies.

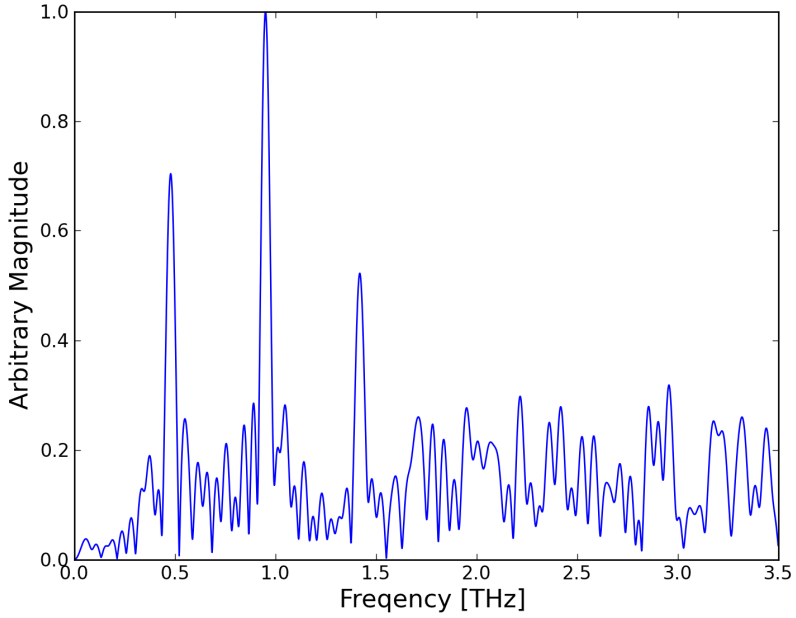

Figure 3.7: Fourier analysis on raw absorped data for comparison

The difference between Figure 3.6 and Figure 3.7 is that the frequency components at $1[THz]$ and $1.5[THz]$ which are strong in Figure 3.7 get smoothened and are not present in the analysis on the filtered data, Figure 3.6.

3.3 Frequency Mapping

Next we investigate two cases. The first one is where the voltage is kept constant at $1[V]$ and the gap spacing of the system is varied from $0.5[\mu m]$ to $4.0[\mu m]$ in steps of $0.5[\mu m]$. A plot of the $\frac{V}{D}\left[\frac{V}{\mu m}\right]$ versus dominant frequency is shown in Figure 3.8.
This is repeated with the gap spacing kept constant a $2[\mu m]$ while the voltage is varied from $0.5[V]$ to $4[V]$ in steps of $0.5[V]$.

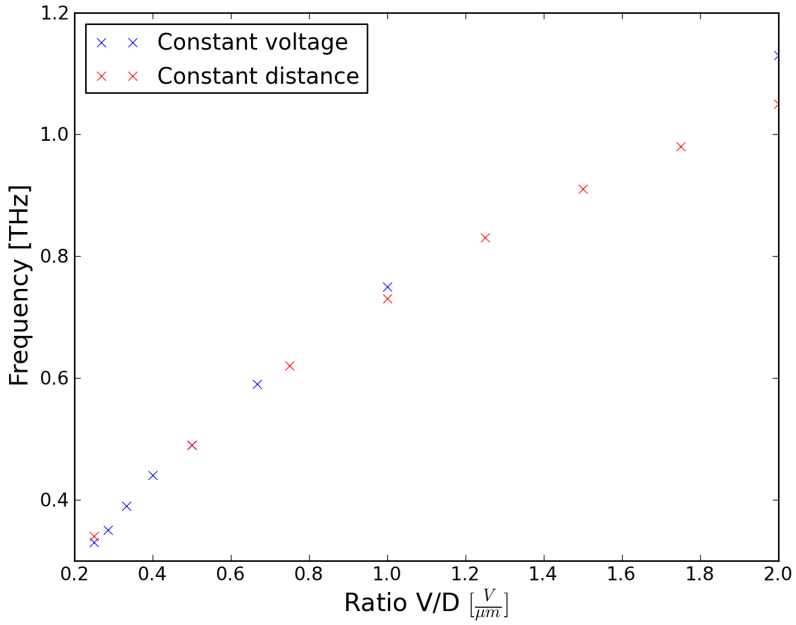

Figure 3.8: Frequency mapping

The x-axis ratio is the applied electric field in the system. As the electric field strength is increased the frequency of the system increases. This agrees with [7]. Although the data doesn't show the exact same value everywhere the difference is negligibe. For the case of $V = 1[V]$ and $d = 2[\mu m]$ the results can't be told apart.

To help visualizing the results Figure 3.9 shows a surface plot of the voltage, distance and frequency.

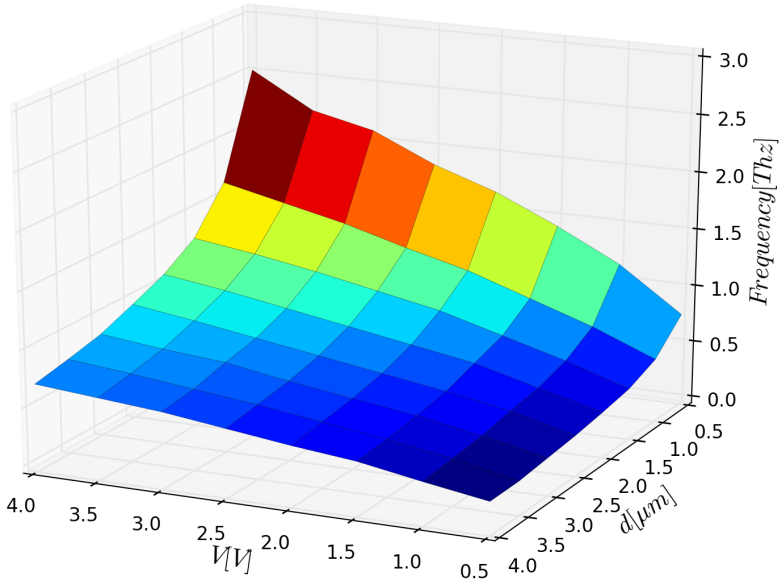

Figure 3.9: Surface plot

Although Figure 3.9 has been turned so that the surface is all visible it's still possible to see that if d is kept constant and V increased the frequency increases and follows the same shape as Figure 3.8.

Figure 3.8 enables direct comparison to Figure 4 in research by Andreas et al.[7] but a more comprehensive plot for all possible combinations is shown in Figure 3.10.

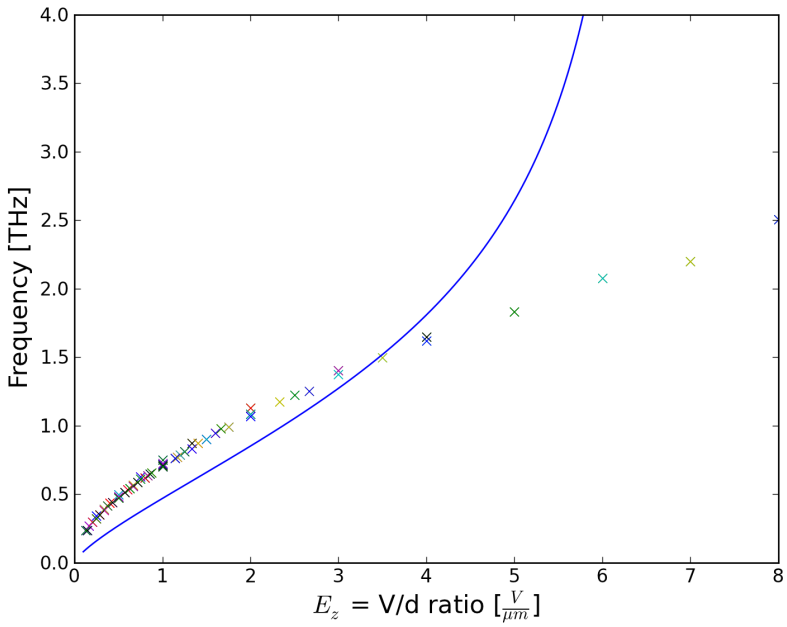

Figure 3.10: Frequency mapping for all available parameters. Blue line is a fit of Equation (3.1).

This Figure is not meant to demonstrate results of specific combinations but the trend of all combinations available. Again there are some glitches in the pattern but majority of the data suggests that there is a strong trend in the signal.

An equation describing the relationship between external electric field and frequency was derived by Pedersen et al.[7].

$$f = \sqrt{\frac{e \cdot E_z}{2 \cdot m_e \cdot R}} \cdot \frac{[1 - (1 - E_z/E_0)^2]^{\frac{1}{4}}}{(1 - E_z/E_0)^{\frac{1}{2}}} \tag{3.1}$$

In calculating the fit, data where the voltage was kept constant at $2[V]$ and the gap length varied from $0.5[\mu m]$ to $4[\mu m]$ was chosen as a reference. Then Equation (3.1) minimized and the error between the result and reference data minimized using least squares.

3.4 Initial Velocity (5%)

Until now every run has been with zero initial velocity. We introduce initial velocity by emitting electrons with maximum emission energy up to 5% of the final energy and running the same analysis as before. Simulations were run longer and because of that the data vectors were too large and the beginning of the data was discarded. This results in the initial peaks not being shown in figures. A zoom in on the smoothed emitted data is shown in Figure 3.13

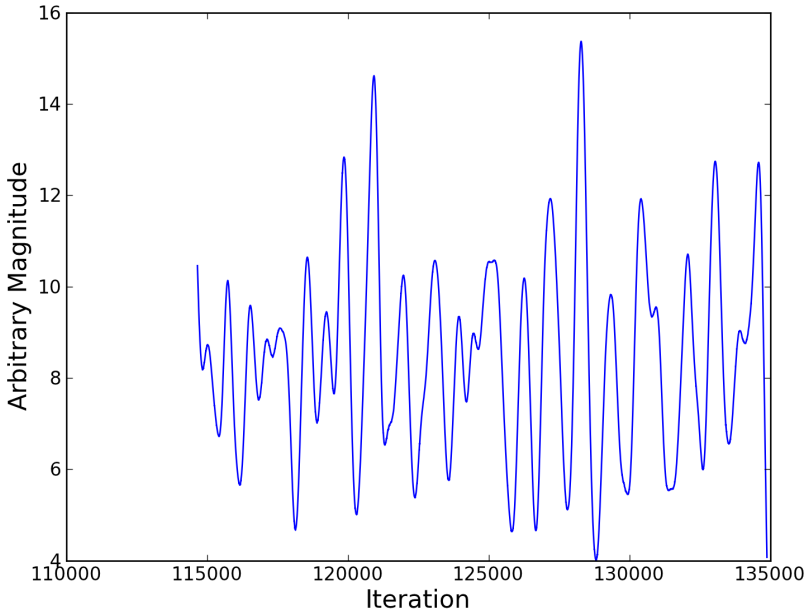

Figure 3.11: Emission with initial velocity (5%)

Comparison with Figure 3.2 shows that forthis distribution of initial velocity the pulses are not as well defined as before. Another observation is that the emission never goes down to zero as in Figure 3.2. This was thought to be because the sigma for the smoothing function was too large relative to the width of the pulses but changing the width to $50[fs]$ and even $15[fs]$ didn't show clear pulses.

To confirm these observations a Fourier analysis of the emission process is shown in Figure 3.12.

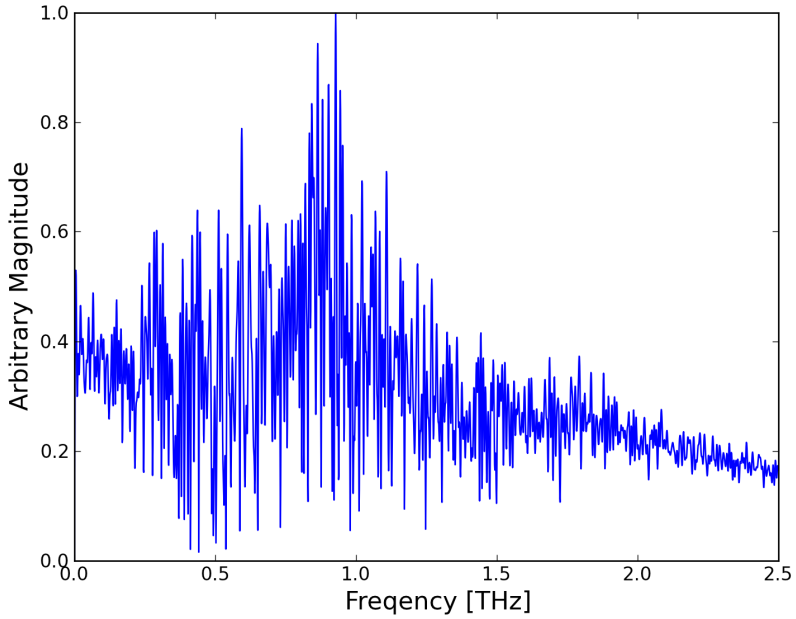

Figure 3.12: Fourier analysis on smoothened emission with initial velocity (5%)

There seem to be some frequency components at around $1[THz]$ but they're not well defined. Previously the peak frequency for emission appeared at $\approx 0.5[THz]$.

Figure 3.13 shows a zoom in on the absorbed smoothened data.

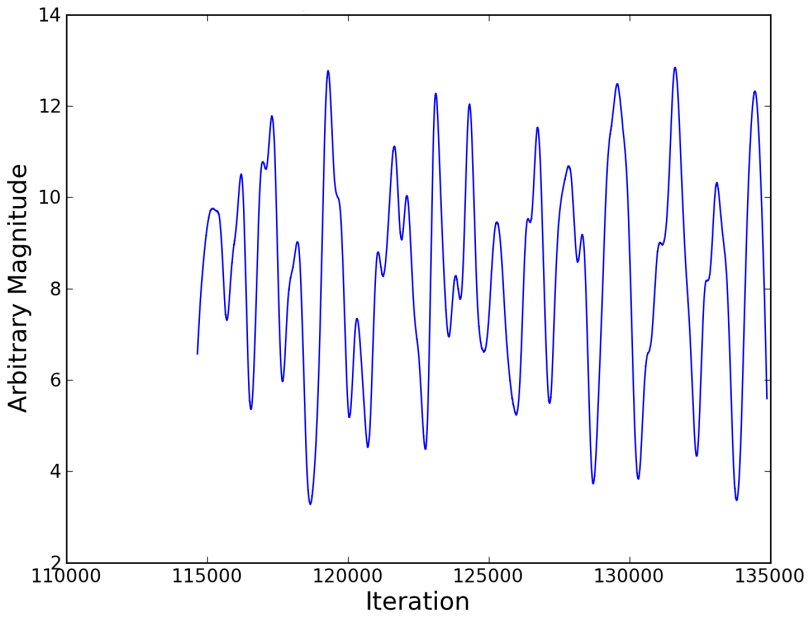

Figure 3.13: Absorption with initial velocity (5%)

Again comparison with the results without initial velocity, Figure 3.5, shows much worse pulsing, if any. The x-axis scaling is automatic resulting in a empty space in the beginning but that has no effects on the analysis.

Finally a frequency analysis of the absorbed data is shown in Figure 3.14.

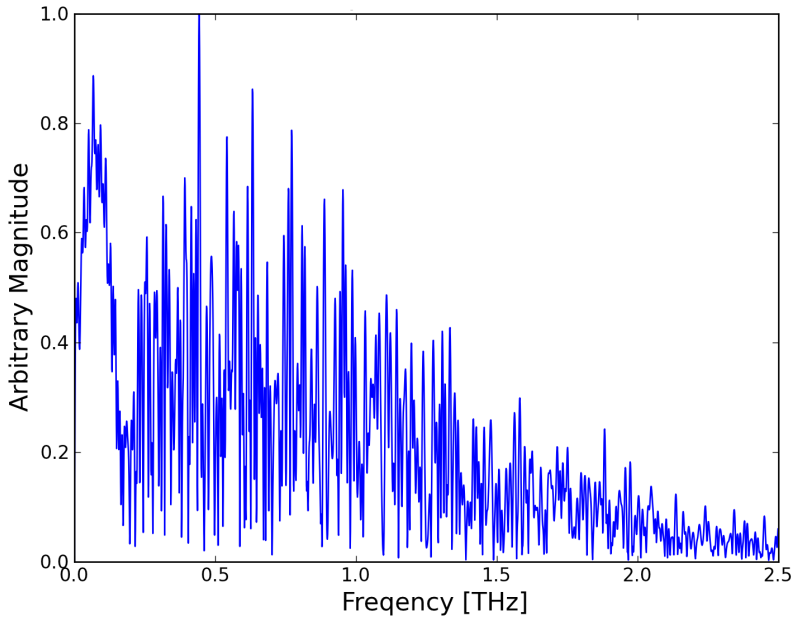

Figure 3.14: Fourier analysis on smoothened absorption with initial velocity (5%)

The fourier analysis shows a lot of noise. Even though the main peak is at about the same frequency as before the signal is very noisy. The behaviour at the beginning is hard to explain as this figure is created the exactly same was as before. This indicates that a practical device is unlikely to function well at cathode temperature corresponding to $0.05[eV]$.

3.5 Initial Velocity (1%)

We now examine the case where the emission energy is up to 1% of the final kinetic energy. After changing the σ of the smoothing filter back and forth ending at $\sigma = 50[fs]$ the results are essentially the same as with initial velocity of 5%.

Figure 3.17 shows the emission data after smoothing.

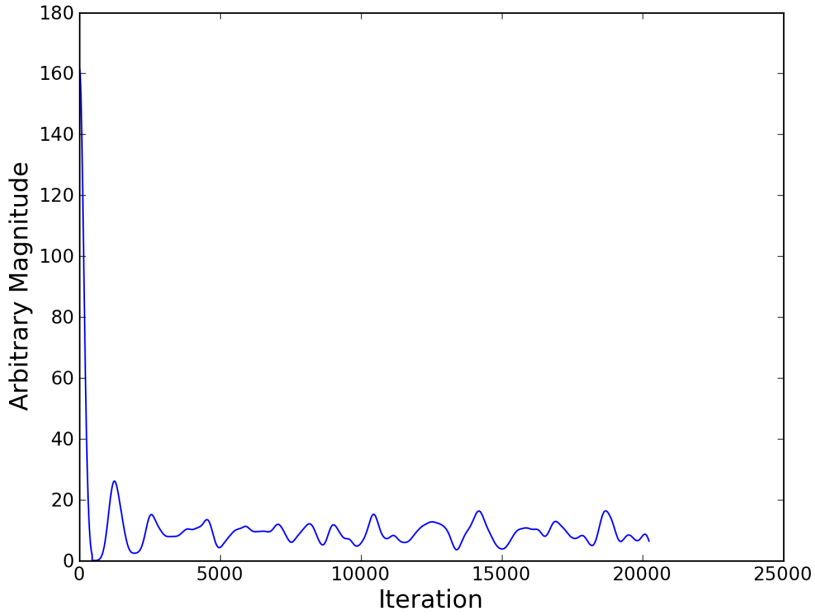

Figure 3.15: Emission with initial velocity (1%)

Comparison with Figure 3.2 shows no definite pulses.

Once again the fourier analysis of the emission process is shown in Figure 3.16.

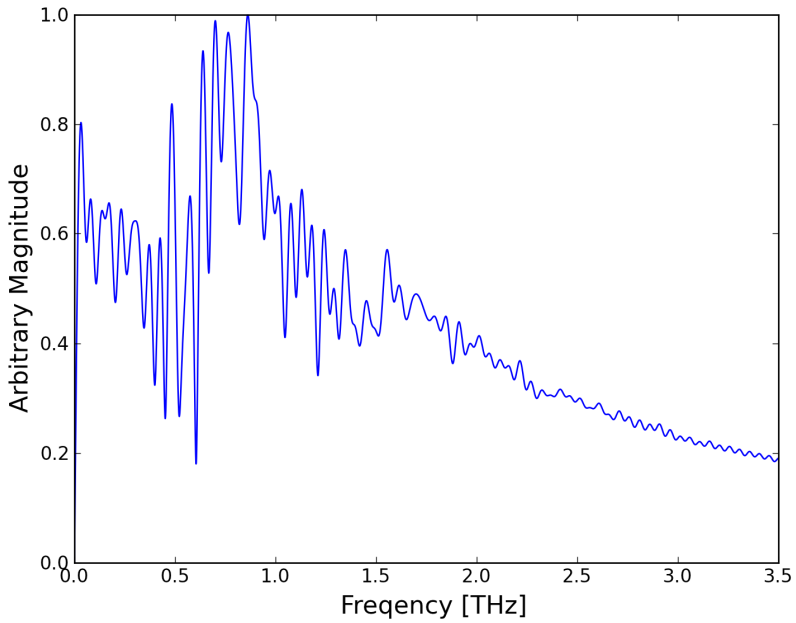

Figure 3.16: Fourier analysis on smoothened emission with initial velocity (1%)

In previous sections the emission process has been very well defined but not in this case. A zoom in on the smoothened absorbtion data is shown next.

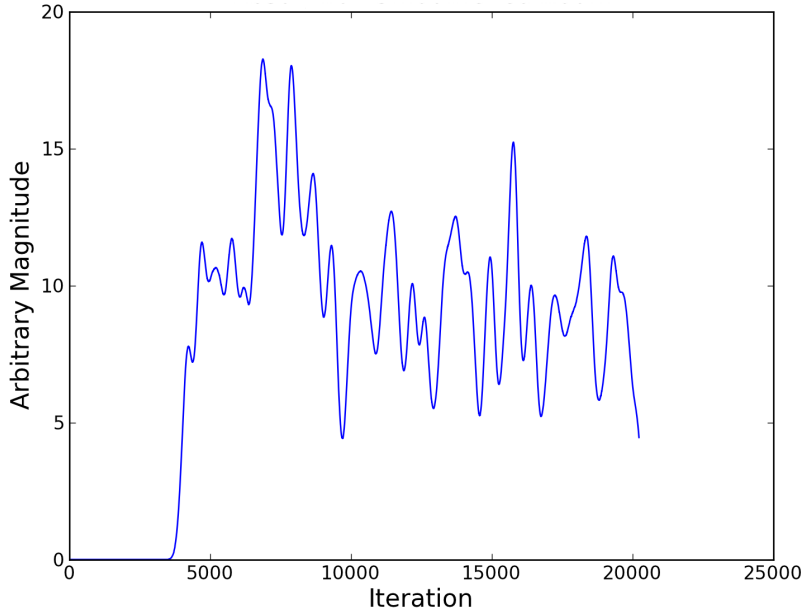

Figure 3.17: Absorption with initial velocity (1%)

Finally a frequency analysis of the absorbed data is shown in Figure 3.18.

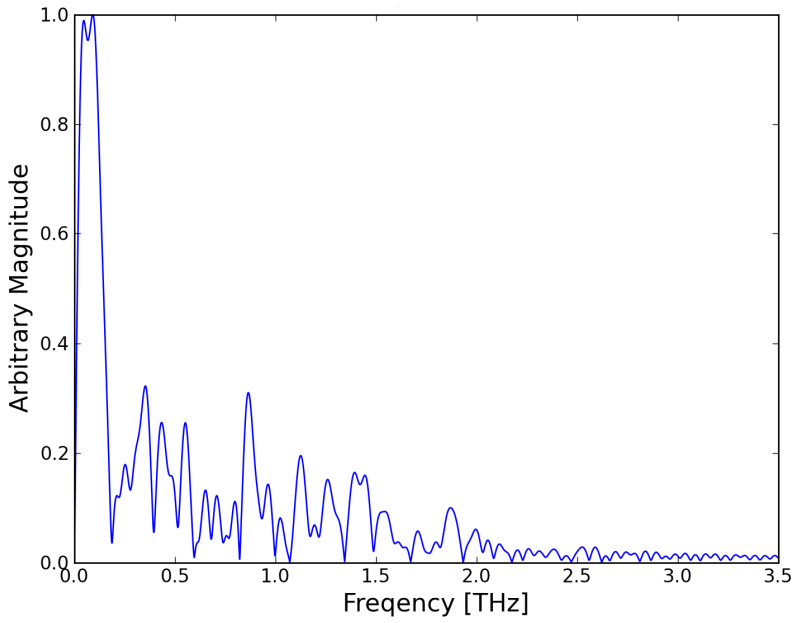

Figure 3.18: Fourier analysis on smoothened absorption with initial velocity (1%)

It's hard to see whether this shows a low frequency component or if the absorption is becoming continuous.

3.6 Smaller timestep

Running the first simulation with smaller timestep is shown here. The data has already been analysed so the plots will be presented with minimal explaination.

3.7 Emission

The raw emission data looks as before

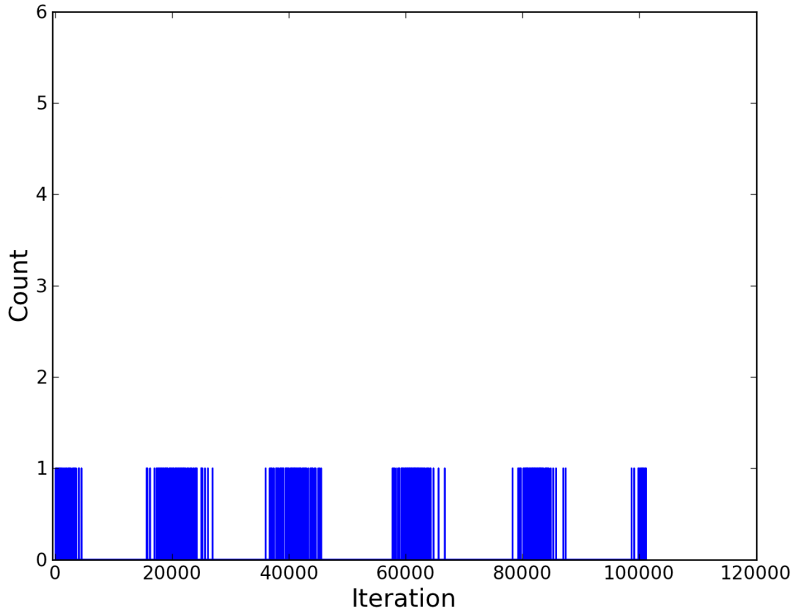

Figure 3.19: Raw emission for timestep of $0.1[fs]$. Same clustering is shown as in Figure 3.1.

As before there is clear clustering. Smoothing this data results in Figure 3.20.

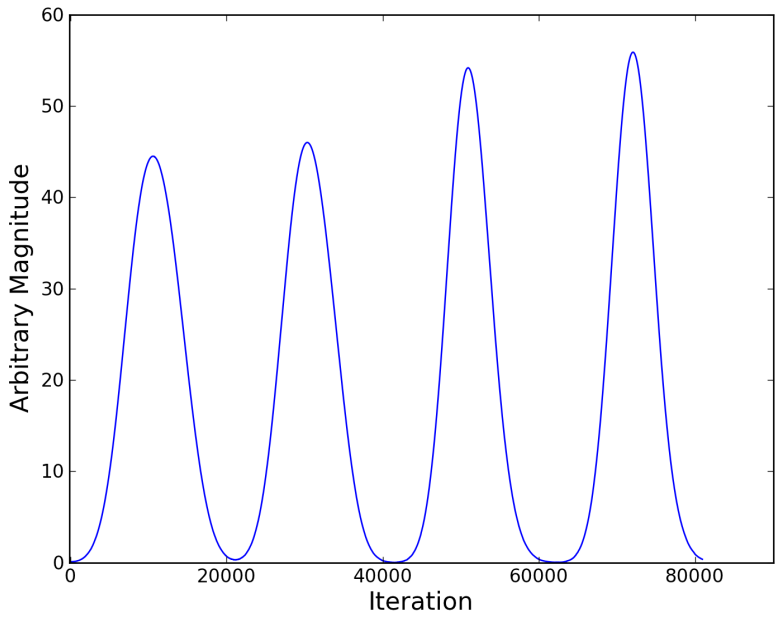

Figure 3.20: Filtered emitted data for smaller timestep showing clear pulsing.

Again a clear clustering is observed. Fourier analysis is shown in Figures 3.21 and 3.22.

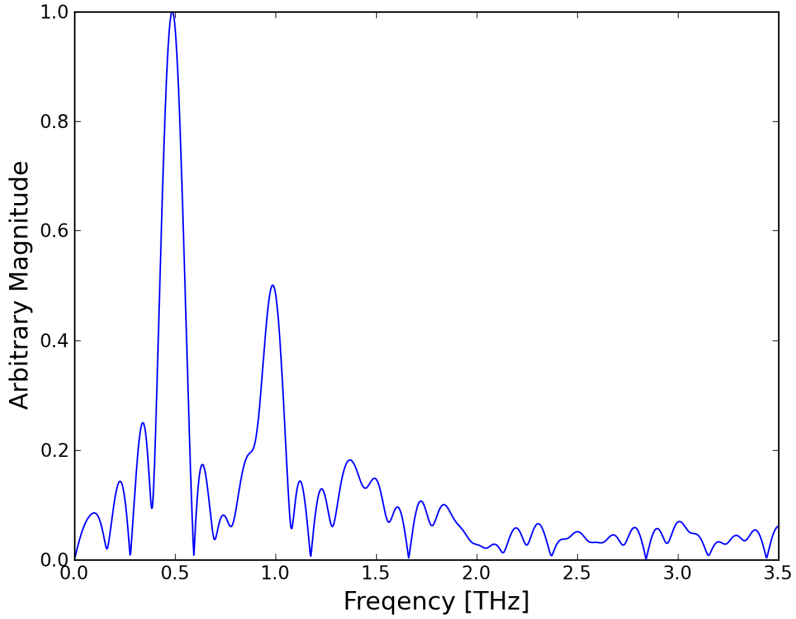

Figure 3.21: Fourier analysis on raw emitted data for smaller timestep confirming results of Figure 3.4

This shows clear and well defined peak at $0.5[THz]$. The peaks above $0.5[THz]$ have lower magnitude than for the original raw data. The frequency component which is

present in Figure 3.4 at $1.5[THz]$ is no longer present indicating that higher resolution may be needed. Analysis of the filtered data is shown next.

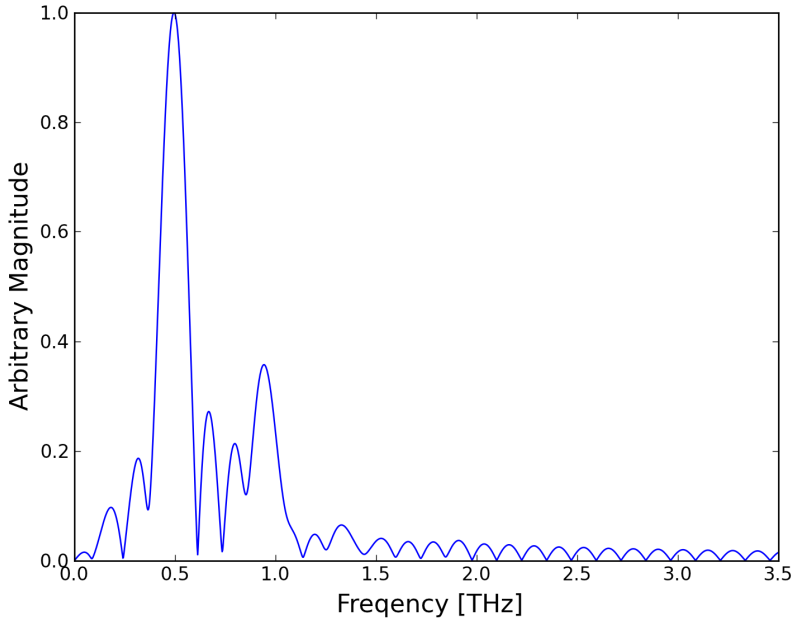

Figure 3.22: Fourir analysis of filtered emitted data for a smaller timestep.

As before the high frequency component magnitude decreases with filtering.

3.8 Absorption

To keep the format the same all the same plots are shown for the absorption. Firstly the raw absorbed data. Nothing can be seen from this graph.

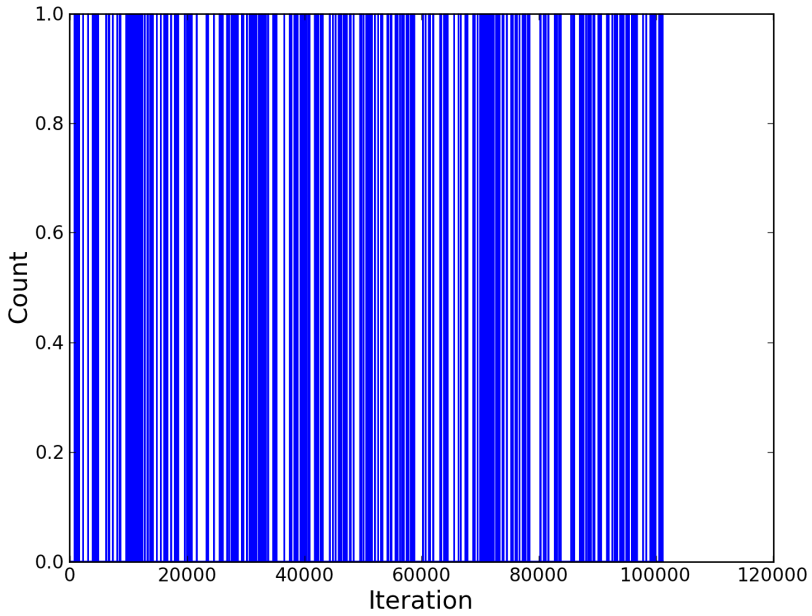

Figure 3.23: Absorption raw for smaller timestep. No clustering is visible.

Smoothing the data as before results in Figure 3.24

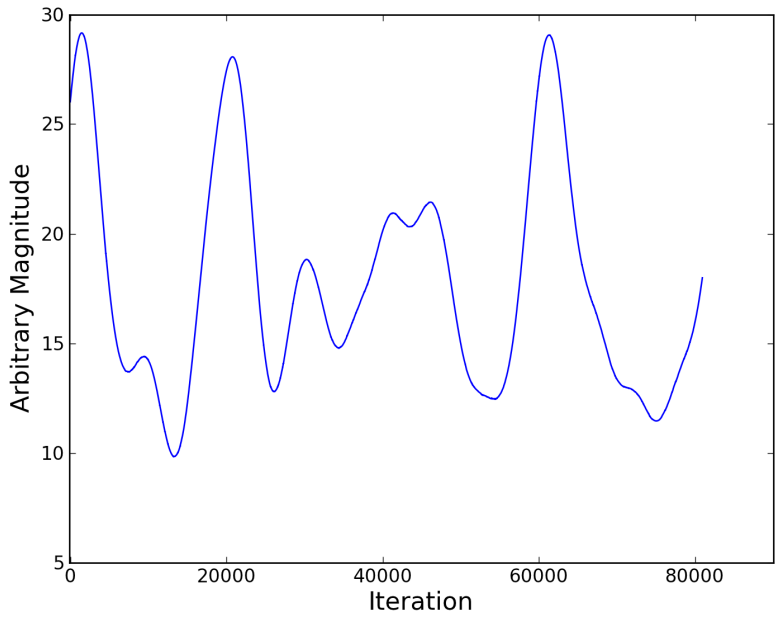

Figure 3.24: Absorption smoothened for smaller timestep. Here some oscillations are shown although they aren't very clear.

Fourier analysis of this data is shown next in Figure 3.25.

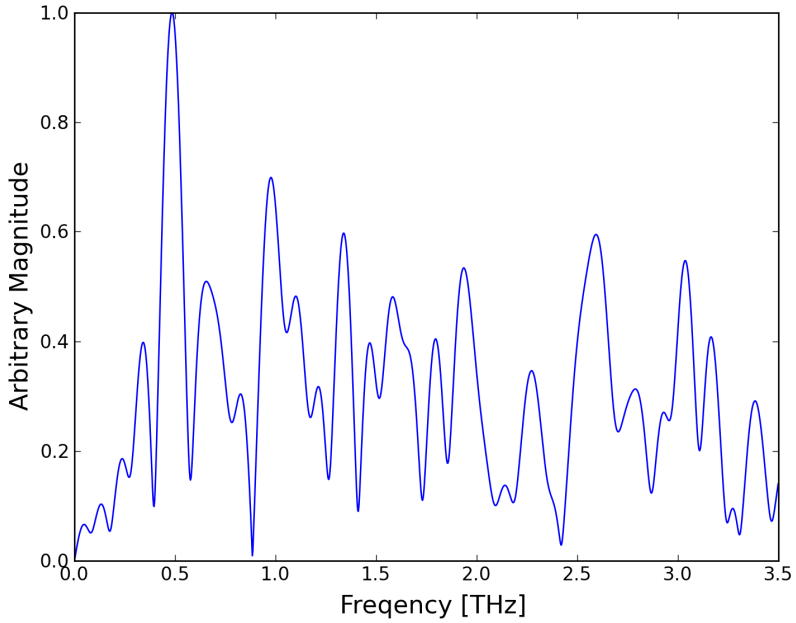

Figure 3.25: Fourier analysis on raw absorbed data for smaller timestep. Noisy signal observed with no dominant frequency component.

Here we see more noise than for the original case. If absorption happens instantaneously then this setup doesn't result in a useful diode.

Fourir analysis for the smoothened absorbed data however shows better results.

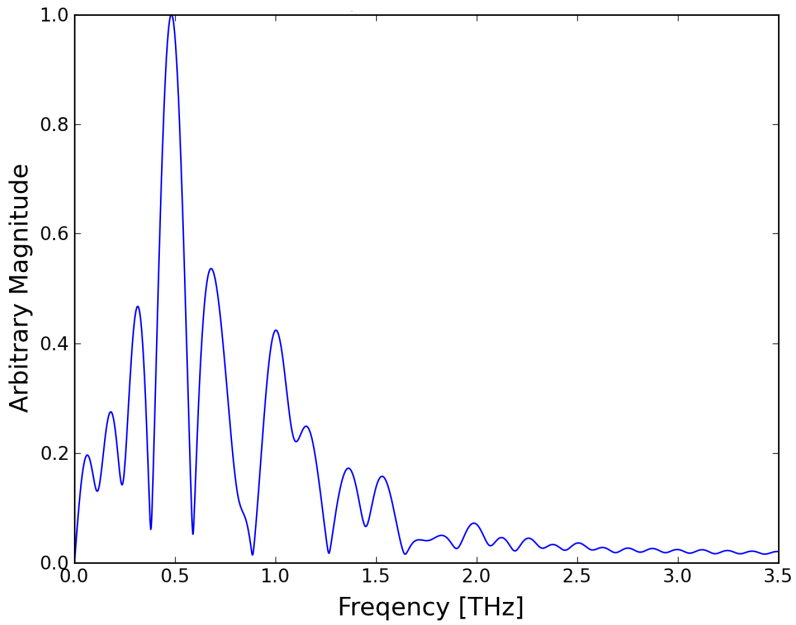

Figure 3.26: Fourier analysis on smoothened absorbed data for smaller timestep. Here again a strong frequency component at $0.5[THz]$ is observed.

Here again we see a strong frequency component at $0.5[THz]$. There frequencies around the main component have higher magnitude than in Figure 3.6 but still a clear dominant frequency.

Chapter 4

Summary

It's hard to simulate every physical aspect of microdiodes and simplifications have to be done and have been in the past with methods such as PIC. This thesis explored the behaviour of a vacuum microdiode with and without initial velocity and confirmed earlier research [7] using the same assumptions and restrictions. Attempts to go further and map parameters as well as removing certain restrictions on the initial system were made with little success. Further research into vacuum microdiodes with initial velocity is needed as well as better understanding of the way an electron is absorped into the anode. Additionally it seems that the diode would have to be cooled to minimize the effects of initial velocity. Increasing the resolution showed similar results although there weren't as clear frequencies at $1.0[Thz]$ and $1.5[THz]$ as before.

With computers becoming more powerful an extremely accurate simulation of microscopic physical systems is possible. The most computationally expensive component of the simulation is the Coulumb force calculation which was parallellized and run on a Intel Core i7 processor but can be run in larger clusters of computers. Although this kind of simulation would benefit more using a faster processor than many cores as the number of electrons in the system at any given time was small.

Bibliography

[1] David Ascher, Paul F. Dubois, Konrad Hinsen, James Hugunin, and Travis Oliphant. *Numerical Python*. Lawrence Livermore National Laboratory, Livermore, CA, ucrl-ma-128569 edition, 1999.

[2] R.J. Barker, IEEE Nuclear, and Plasma Sciences Society. *Modern microwave and millimeter-wave power electronics*. IEEE Press, 2005.

[3] C.K. Birdsall. Particle-in-cell charged-particle simulations, plus monte carlo collisions with neutral atoms, pic-mcc. *IEEE Transactions on Plasma Science*, 1991.

[4] Jonathan Dummer. . [online] `http://lonesock.net/article/verlet.html`.

[5] J.A. Eichmeier and M. Thumm. *Vacuum Electronics: Components and Devices*. Springer, 2010.

[6] Particle in Cell Consulting LLC. The Electrostatic Particle In Cell (ES-PIC) Method, 2010. [online] `http://www.particleincell.com/2010/es-pic-method/`.

[7] Andreas Pedersen, Andrei Manolescu, and Ágúst Valfells. Space-charge modulation in vacuum microdiodes at thz frequencies. *Phys. Rev. Lett.*, 104:175002, Apr 2010.

[8] H.D. Young, R.A. Freedman, and A.L. Ford. *Sears and Zemansky's University Physics: With Modern Physics*. MasteringPhysics Series. Pearson Addison Wesley, 2004.

[9] W. Zhu. *Vacuum Microelectronics*. Wiley, 2001.

Appendix A

Program options

Since this program is to be a research tool it has to have flexibility and possibility to run for a variety of different preferences. Therefor a simple file with all options was kept seperate from the functions where constants are defined and options can be chosen, usually as either some value or a boolean. The following options, shown in Table Table A.1, are currently available but it's quite simple to add new functionality.

	Type	Default Value
TimeStep	Number	$1 \cdot 10^{-15}[s]$
Initial Position	Number	$1 \cdot 10^{-9}[m]$
Initial Velocity	Boolean	3
Radius of Cathode	Number	$250 \cdot 10^{-9}[m]$
Confining Electric Field	Boolean	0
Initial Velocity	Boolean	0
Initial Velocity (Relative to max kinetic energy)	Fraction	0.01 (1%)
Initial Velocity Distribution (Uniform Velocity distribution = 1) (Uniform Energy distribution = 0)	Boolean	1
Iterations (How many times the v.t.t. should the program run	Integer	10

Table A.1: Program Options

Some explaination is due here. Uniform velocity distribution and uniform energy distribution are mutually exclusive, i.e. you chose one of the two. The vacuum transit time (v.t.t.) is the number of iterations it takes a single electron injected into the system with zero intital velocity to escape the system at the anode. Iteration is a multiply of v.t.t. and is constructed in this way to ensure that the program runs long enough. This time is

larger than in reality as Columb forces from electrons act to accelerate the first electron so that she escapes before this calculated v.t.t. iterations comes. It is possible though to use this as an rough estimate of how many „sheets" go through the system. Choosing 10 for the „Iterations" we can assume that about 10 sheets are emitted and travel through the system.

School of Science and Engineering
Reykjavík University
Menntavegur 1
101 Reykjavík, Iceland
Tel. +354 599 6200
Fax +354 599 6201
www.reykjavikuniversity.is
ISSN 1670-8539